

The parton branching method for TMD evolution and applications at the LHC

Informal Science Coffee 9 February 2021

Mees van Kampen



LUNDS
UNIVERSITET



Universiteit
Antwerpen



Why Transverse Momentum Dependent PDFs (TMDs)?

1. Accurately describe the Z boson q_T spectrum @low- q_T

- High- q_T : fixed order QCD calculation
- Low- q_T : enhanced terms

$$\alpha_s^n \ln^m Q/q_T$$

destroy perturbative series in $\alpha_s \rightarrow$ need resummation in generalized form of QCD factorization: low- q_T factorization.

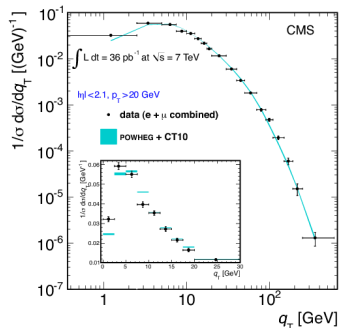


Figure 1: Z boson transverse momentum spectrum by POWHEG. Angeles-Martinez et al. 1507.05267v1

Why Transverse Momentum Dependent PDFs?

2. Proton's structure functions at small x

- High energies $\sqrt{s} \gg M$ at the LHC, enhanced terms

$$(\alpha_s \ln \sqrt{s}/M)^n$$

need resummation.

- **High energy** $\sqrt{s} \rightarrow$ many small x events. At low **longitudinal** momenta, the fraction of momentum by **transverse** degrees of freedom becomes more important

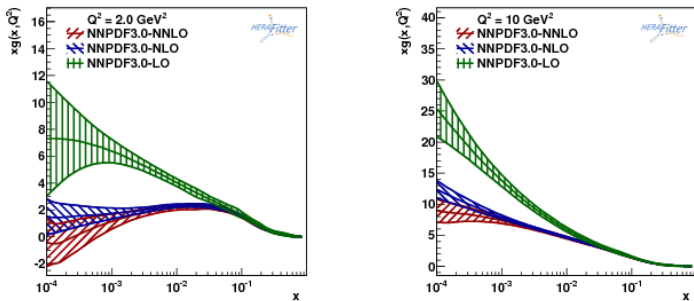


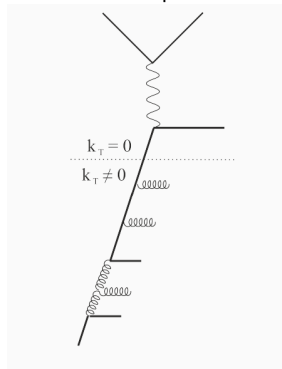
Figure 2: gluon PDFs as function of longitudinal momentum fraction x
Angeles-Martinez et al. 1507.05267v1

Parton branching method

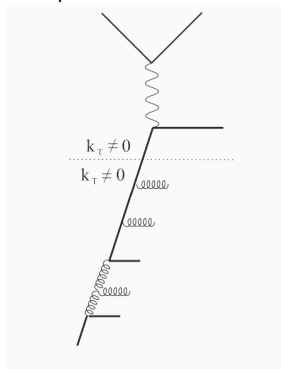
Motivation for the Parton Branching method

Treat transverse momentum kinematics without any mismatch between the hard (matrix element) and soft (parton shower) parts.

Standard MC predictions



MC predictions with TMDs



Goal of PB: Construct an iterative evolution for TMDs in wide kinematic range by taking into account the **transverse momentum at each branching**.

The Parton Branching (PB) method

TMDs should obey RG invariance and generalize evolution of collinear PDFs. This is satisfied in the DGLAP evolution equation:

$$\frac{\partial \tilde{f}_a(x, \mu^2)}{\partial \ln \mu^2} = \sum_b \int_x^1 dz \underbrace{P_{ab}(\alpha_s(\mu^2), z)}_{\text{Splitting functions}} \tilde{f}_b\left(\frac{x}{z}, \mu^2\right) \quad (1)$$

Resum soft gluons with the *unitarity approach*:

- 1 **Soft-gluon resolution scale:** z_M
separates resolvable ($z < z_M$) from non-resolvable ($z > z_M$) parton splittings
- 2 **Real splitting functions:** $P_{ab}^{(R)}(\alpha_s(\mu^2), z)$
- 3 **Momentum sum rule:** $\sum_a \int_0^1 dz z P_{ab}(z, \mu^2) = 0$ (and $P_{ab} = P_{ab}^{(R)} + P_{ab}^{(V)}$)
- 4 **Sudakov form factor** for non-resolvable branchings (restoring unitarity):

$$\Delta_a(\mu^2, \mu_0^2) = \exp \left\{ - \sum_b \int_{\mu_0^2}^{\mu^2} \frac{d\mu'^2}{\mu'^2} \int_0^{z_M} dz z P_{ab}^{(R)}(\alpha_s(\mu'^2), z) \right\} \quad (2)$$

[F. Hautmann et al. JHEP 01, 070 (2018) arXiv:1708.03279]

The Parton Branching (PB) method

Rewriting the evolution equation with the real splitting functions $P_{ab}^{(R)}$ and Sudakov Δ_a gives:

$$\frac{\partial}{\partial \ln \mu^2} \left(\frac{\tilde{f}_a(x, \mu^2)}{\Delta_a(\mu^2)} \right) = \sum_b \int_x^{z_M} dz P_{ab}^{(R)}(\alpha_s(\mu^2), z) \frac{\tilde{f}_b(x/z, \mu^2)}{\Delta_a(\mu^2)} \quad (3)$$

Integrate this from μ_0 up to μ :

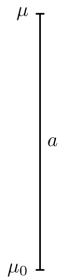
$$\begin{aligned} \tilde{f}_a(x, \mu^2) &= \Delta_a(\mu^2) \tilde{f}_a(x, \mu_0^2) + \\ &+ \sum_b \int_{\mu_0^2}^{\mu^2} \frac{d\mu'^2}{\mu'^2} \int_x^{z_M} dz \frac{\Delta_a(\mu^2)}{\Delta_a(\mu'^2)} P_{ab}^{(R)}(z, \alpha_s(\mu'^2)) \tilde{f}_b\left(\frac{x}{z}, \mu'^2\right). \end{aligned} \quad (4)$$

→ This can be solved iteratively (multiple branchings).

Iterative solution

Iterative solution has an intuitive interpretation with multiple branchings:

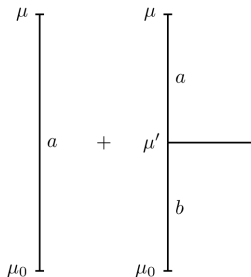
$$\tilde{f}_a(x, \mu^2) = \Delta_a(\mu^2) \tilde{f}_a(x, \mu_0^2) + \dots$$



Iterative solution

Iterative solution has an intuitive interpretation with multiple branchings:

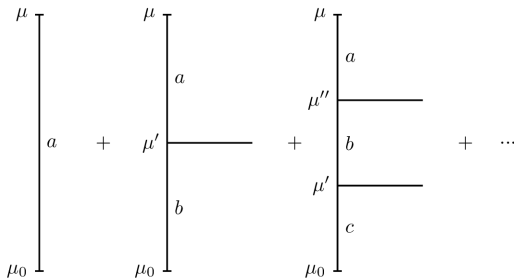
$$\begin{aligned} \tilde{f}_a(x, \mu^2) &= \Delta_a(\mu^2) \tilde{f}_a(x, \mu_0^2) \\ &+ \sum_b \int_{\mu_0^2}^{\mu^2} \frac{d\mu'^2}{\mu'^2} \frac{\Delta_a(\mu^2)}{\Delta_a(\mu'^2)} \int_x^{z_M} dz P_{ab}^{(R)}(z, \alpha_s(\mu'^2)) \Delta_b(\mu'^2) \tilde{f}_b\left(\frac{x}{z}, \mu_0^2\right) + \dots \end{aligned}$$



Iterative solution

Iterative solution has an intuitive interpretation with multiple branchings:

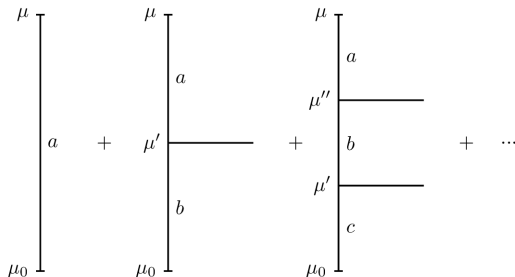
$$\begin{aligned}
 \tilde{f}_a(x, \mu^2) &= \Delta_a(\mu^2) \tilde{f}_a(x, \mu_0^2) \\
 &+ \sum_b \int_{\mu_0^2}^{\mu^2} \frac{d\mu'^2}{\mu'^2} \frac{\Delta_a(\mu'^2)}{\Delta_a(\mu'^2)} \int_x^{z_M} dz P_{ab}^{(R)}(z, \alpha_s(\mu'^2)) \Delta_b(\mu'^2) \tilde{f}_b\left(\frac{x}{z}, \mu_0^2\right) \\
 &+ \sum_{b,c} \int \frac{d\mu''^2}{\mu''^2} \int \frac{d\mu'^2}{\mu'^2} \frac{\Delta_b(\mu'^2)}{\Delta_b(\mu'^2)} \frac{\Delta_a(\mu^2)}{\Delta_a(\mu'^2)} \int_x^{z_M} dz_2 \int_{x/z_2}^{z_M} dz_1 \\
 &\times P_{ab}^{(R)}(\alpha_s(\mu''^2), z_2) P_{bc}^{(R)}(\alpha_s(\mu'^2), z_1) \Delta_c(\mu'^2) \tilde{f}_c\left(\frac{x}{z_1 z_2}, \mu_0^2\right) + \dots
 \end{aligned}$$



Iterative solution

Iterative solution has an intuitive interpretation with multiple branchings:

$$\begin{aligned}
 \tilde{f}_a(x, \mu^2) &= \Delta_a(\mu^2) \tilde{f}_a(x, \mu_0^2) \\
 &+ \sum_b \int_{\mu_0^2}^{\mu^2} \frac{d\mu'^2}{\mu'^2} \frac{\Delta_a(\mu'^2)}{\Delta_a(\mu'^2)} \int_x^{z_M} dz P_{ab}^{(R)}(z, \alpha_s(\mu'^2)) \Delta_b(\mu'^2) \tilde{f}_b\left(\frac{x}{z}, \mu_0^2\right) \\
 &+ \sum_{b,c} \int \frac{d\mu''^2}{\mu''^2} \int \frac{d\mu'^2}{\mu'^2} \frac{\Delta_b(\mu'^2)}{\Delta_b(\mu'^2)} \frac{\Delta_a(\mu^2)}{\Delta_a(\mu'^2)} \int_x^{z_M} dz_2 \int_{x/z_2}^{z_M} dz_1 \\
 &\times P_{ab}^{(R)}(\alpha_s(\mu''^2), z_2) P_{bc}^{(R)}(\alpha_s(\mu'^2), z_1) \Delta_c(\mu'^2) \tilde{f}_c\left(\frac{x}{z_1 z_2}, \mu_0^2\right) + \dots
 \end{aligned}$$



This is done in the uPDFevolv code [arXiv:1407.5935v2].

The PB method for TMDs

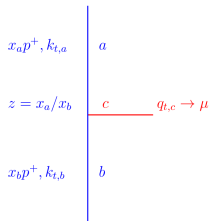
$$\tilde{f}_a(x, \mu) = \int d^2 \mathbf{k}_t \underbrace{\tilde{\mathcal{A}}_a(x, \mathbf{k}_t, \mu)}_{\text{TMD}} \quad (5)$$

PB equation for TMDs $\tilde{\mathcal{A}}_a(x, k_t, \mu)$:

$$\begin{aligned} \tilde{\mathcal{A}}_a(x, \mathbf{k}_t, \mu^2) &= \Delta_a(\mu^2) \tilde{\mathcal{A}}_a(x, \mathbf{k}_t, \mu_0^2) + \\ &+ \sum_b \left[\int \frac{d^2 \mu'}{\pi \mu'^2} \Theta(\mu^2 - \mu'^2) \Theta(\mu'^2 - \mu_0^2) \frac{\Delta_a(\mu^2)}{\Delta_a(\mu'^2)} \right. \\ &\quad \left. \times \int_x^1 dz \Theta(z_M(\mu') - z) P_{ab}^{(R)}(z, \alpha_s(q_\perp)) \tilde{\mathcal{A}}_b\left(\frac{x}{z}, \mathbf{k}_t + \mathbf{q}_{t,c}, \mu'^2\right) \right] \end{aligned} \quad (6)$$

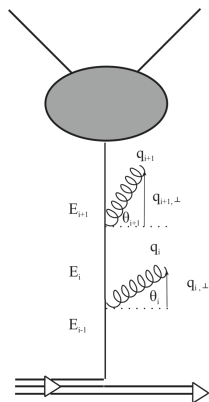
Deal with transverse momentum dependence

- Intrinsic k_t distribution:
 $\tilde{\mathcal{A}}_a(x, k_{t,0}, \mu_0) = f_a(x, \mu_0) \exp(-k_{t,0}^2/\sigma^2)$
- How to calculate q_t using the branching scale μ' ?
- Sum over all transverse momentum:
 $k_t = k_{t,0} - \sum_i q_{t,i}$



Kinematics in each branching governed by momentum conservation: $k_{t,b} = k_{t,a} + q_{t,c}$

Angular ordering condition



- QCD colour coherence: branchings ordered according to their angle θ_i
- Emitted transverse momentum in each branching:

$$|q_{\perp,i}| = (1 - z_i) |k_{i-1}| \sin \theta_i$$

- Associate the evolution variable μ' with the **rescaled transverse momentum** \bar{q}_{\perp} :

$$\mu' = \bar{q}_{\perp} = \frac{q_{\perp}}{1 - z} \quad (7)$$

⇒ **angular ordering** condition

- Calculation of k_{i+1} from k_i : $k_{i+1} = k_i - (1 - z_i)\mu'$
- Soft-gluon resolution scale with (7) becomes μ' -dependent:

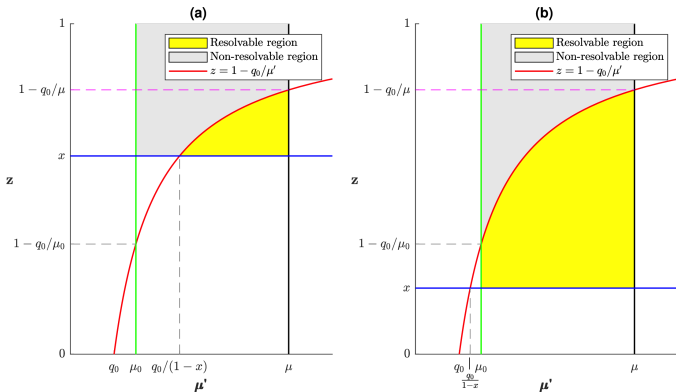
$$z_M(\mu') = \max \left(1 - \frac{q_{\perp}}{\mu'} \right) = 1 - \frac{q_0}{\mu'} \quad (q_0 = q_{\perp, \min})$$

- Scale in strong coupling: $\alpha_s(q_{\perp}^2) = \alpha_s((1 - z)^2 \mu'^2)$

Dynamical resolution scale $z_M(\mu')$

[Hautmann, Lelek, Keersmaekers, MvK, arXiv:1908.08524]

(μ', z) -space



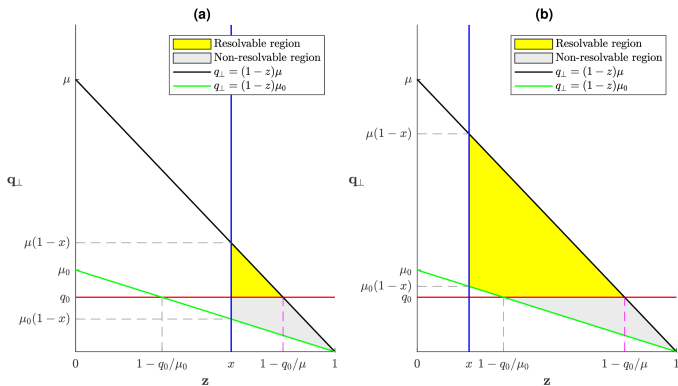
- z_M depends on μ' according to angular ordering
- scale q_0 influences borders of resolvable region and avoids the Landau pole ($\alpha_s(q_\perp^2)$)!
- two scenarios depending on the value of x

Dynamical resolution scale $z_M(\mu')$

[Hautmann, Lelek, Keersmaekers, MvK, arXiv:1908.08524]

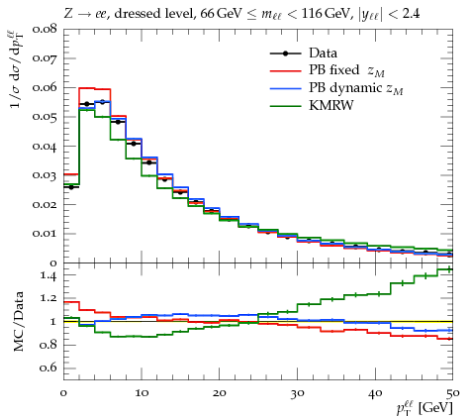
Transformation from scale μ' to transverse momentum q_{\perp} .

(z, q_{\perp}) -space



Z boson p_T spectrum with dynamical z_M

- Compare simulations with LHC data (ATLAS, $\sqrt{s} = 8$ GeV [Eur.Phys.J. C76 (2016) no.5, 291])
- Compare PB fixed z_M with PB dynamical z_M



- Shape is better described at low p_T using the dynamical resolution scale

Backward evolution with PB method

- Z p_T : only TMD input is enough (no shower needed)
- For Z + jets: **parton shower** is necessary

The evolution equation for TMDs:

$$\frac{\partial}{\partial \ln \mu^2} \left(\frac{\tilde{\mathcal{A}}_a(x, k_t, \mu)}{\Delta_a(\mu)} \right) = \sum_b \int_x^{z_M} dz \frac{d\phi}{2\pi} P_{ab}^{(R)} \frac{\tilde{\mathcal{A}}_b(x/z, k'_t, \mu)}{\Delta_a(\mu)},$$

normalize to $\frac{\tilde{\mathcal{A}}_a(x, k_t, \mu)}{\Delta_a(\mu)}$:

$$\frac{\Delta_a(\mu)}{\tilde{\mathcal{A}}_a(x, k_t, \mu)} d \left(\frac{\tilde{\mathcal{A}}_a(x, k_t, \mu)}{\Delta_a(\mu)} \right) = \sum_b \frac{d\mu^2}{\mu^2} \int_x^{z_M} dz \frac{d\phi}{2\pi} P_{ab}^{(R)} \frac{\tilde{\mathcal{A}}_b(x/z, k'_t, \mu)}{\tilde{\mathcal{A}}_a(x, k_t, \mu)},$$

and integrate over μ' from μ_i down to μ_{i-1} to obtain:

$$\Delta_{bw}(x, k_t, \mu_i, \mu_{i-1}) = \exp \left\{ - \sum_b \int_{\mu_{i-1}^2}^{\mu_i^2} \frac{d\mu'^2}{\mu'^2} \int_x^{z_M} dz P_{ab}^{(R)} \frac{\tilde{\mathcal{A}}_b(x/z, k'_t, \mu')}{\tilde{\mathcal{A}}_a(x, k_t, \mu')} \right\}.$$

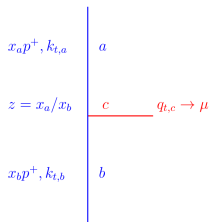
This Sudakov is used as the **no-branching probability** in the TMD parton shower.

Implementations in Cascade

No-branching probability with TMDs!

$$\Delta_{bw}(x, k_t, \mu_i, \mu_{i-1}) = \exp \left\{ - \sum_b \int_{\mu_{i-1}^2}^{\mu_i^2} \frac{d\mu'^2}{\mu'^2} \int_x^{z_M} dz P_{ab}^{(R)} \frac{\tilde{\mathcal{A}}_b(x/z, k'_t, \mu')}{\tilde{\mathcal{A}}_a(x, k_t, \mu')} \right\}.$$

TMD parton shower:



- Determine branching scale with $\Delta_{bw}(x, k_t, \mu_i, \mu_{i-1})$
- In each splitting

$$k_{t,b} = k_{t,a} + (1 - z)\mu$$

- Total transverse momentum:

$$k_{\perp} = k_{\perp,0} - \sum_c q_{t,c}$$

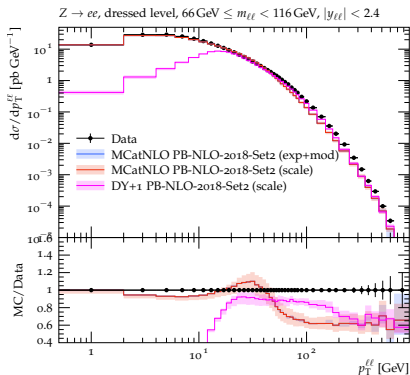
This is implemented in the Monte Carlo event generator CASCADE [arXiv:2101.10221v1].

Some features:

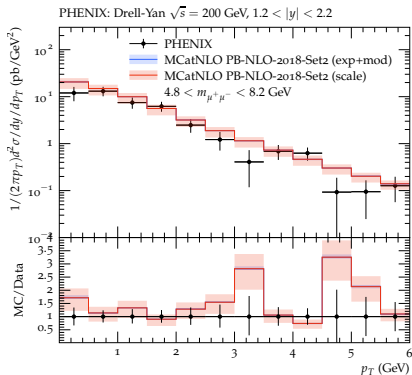
- TMDs as input
- PB based parton shower that follows dynamics of the input TMD
- Possibility for off-shell matrix elements

Achievements of the PB method

- TMD sets fitted to data
- Matched with NLO matrix element from Madgraph_aMC@NLO
- Good description of DY p_T spectrum at both low and high DY mass



Z p_T spectrum from NLO ME combined with a PB TMD in Cascade. Data from ATLAS at $\sqrt{s} = 8 \text{ TeV}$. [arXiv:1906.00919v2]



Drell Yan p_T spectrum in a low mass window. Data from PHENIX at $\sqrt{s} = 200 \text{ GeV}$. [arXiv:2001.06488v1]

Comparison Parton branching with CSS resummation

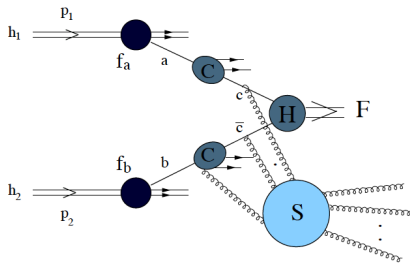
The CSS formalism

Well-established formalism that provides an analytical expression for inclusive processes:
 $h_1(p_1) + h_2(p_2) \rightarrow F(M, q_\perp) + X$

$$\frac{d\sigma}{dQ^2 dy d\mathbf{q}_\perp^2} \simeq \int d^2\mathbf{b} e^{i\mathbf{b}\cdot\mathbf{q}_\perp} \frac{\sigma^{(0)}}{s} \sum_{a,b} \mathcal{F}_{a/A}(\mathbf{b}; Q, \xi_a, \mu) \mathcal{F}_{b/B}(\mathbf{b}; Q, \xi_b, \mu) + Y(\mathbf{q}_\perp; Q, x_a, x_b)$$

TMDs from CSS are factorized in PDFs, coefficient functions and Sudakov form factor:

$$\mathcal{F}_{q/i} \sim f_{q/i} \otimes C_{jq} \otimes \sqrt{S}$$



The CSS and PB Sudakov form factors

CSS' Sudakov:

$$\sqrt{S(Q^2, b^2)} = \exp \left(-\frac{1}{2} \int_{1/b^2}^{Q^2} \frac{d\mu^2}{\mu^2} \left[\ln \left(\frac{Q^2}{\mu^2} \right) A_a(\alpha_s(\mu^2)) + B_a(\alpha_s(\mu^2)) \right] \right)$$

PB Sudakov:

$$\Delta_a(\mu^2, \mu_0^2) \approx \exp \left(- \int \frac{dq_{\perp}^2}{q_{\perp}^2} \left[\frac{1}{2} \ln \left(\frac{\mu^2}{q_{\perp}^2} \right) k_a(\alpha_s(q_{\perp}^2)) - d_a(\alpha_s(q_{\perp}^2)) \right] \right)$$

A , B , k and d have perturbative expansions in α_s :

$$A_a(\alpha_s) = \sum_{n=1}^{\infty} \left(\frac{\alpha_s}{\pi} \right)^n A_a^{(n)}, \quad k_a(\alpha_s) = \sum_{n=1}^{\infty} \left(\frac{\alpha_s}{2\pi} \right)^n k_a^{(n-1)}$$

Logarithmic counting of resummation of $\alpha_s^n \ln^m(Q^2/q_T^2)$ terms as:

- leading logarithmic (LL) accuracy $\alpha_s^n \ln^{n+1}(Q^2/q_T^2)$
- next-to-leading logarithmic (NLL) accuracy $\alpha_s^n \ln^n(Q^2/q_T^2)$
- next-to-next-to-leading logarithmic (NNLL) accuracy $\alpha_s^n \ln^{n-1}(Q^2/q_T^2)$

Analytical comparison CSS and PB

[de Florian, Grazzini; Phys.Rev.Lett. 85 (2000) 4678-4681]

[Hautmann et al.; JHEP 01 (2018) 070]

$$A_a^{(n)} \stackrel{?}{=} \frac{1}{2^n} k_a^{(n-1)}$$

$$B_a^{(n)} \stackrel{?}{=} -\frac{1}{2^{n-1}} d_a^{(n-1)}$$

- LL:

$$A_q^{(1)} = C_F,$$

$$k_q^{(0)} = 2C_F$$

- NLL:

$$A_q^{(2)} = \frac{1}{2} C_F C_A \left(\frac{67}{18} - \frac{\pi^2}{6} \right) - \frac{5}{18} N_f C_F$$

$$B_q^{(1)} = -\frac{3}{2} C_F$$

$$k_q^{(1)} = 2C_F C_A \left(\frac{67}{18} - \frac{\pi^2}{6} \right) - \frac{10}{9} N_f C_F$$

$$d_q^{(0)} = \frac{3}{2} C_F$$

- NNLL: Differences observed

- ▶ Hard function H and B coefficient are connected by renormalization group transformation:

$$H^F(\alpha_s(Q^2)) = \underbrace{\exp \left\{ \int_{c_0/b^2}^{Q^2} \frac{d\mu^2}{\mu^2} \gamma_H(\alpha_s(\mu^2)) \right\}}_{\text{in Sudakov}} H^F(\alpha_s(c_0/b^2)).$$

- ▶ $A^{(3)}$ relates to the soft-gluon effective coupling
- ▶ $k^{(2)}$ is cusp anomalous dimension, missing terms for effective coupling

[F. Coradeschi, T. Cridge; Comput.Phys.Commun. 238 (2019) 262-294]

reSolve is a recently developed semi-analytical program that implements CSS resummation.

- Only resummation part, no matching to finite terms yet
- Calculations up to NNLL accuracy
- Three scales: μ_F, μ_R, μ_S
- Non-perturbative parameterization for the resummed part with a Gaussian smearing factor:

$$G_i^{NP} = \exp\{-g_i^{NP} b^2\}$$

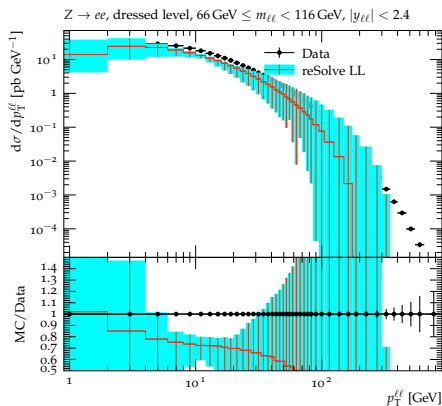
Aim of both the PB and CSS communities is to increase precision in predictions for LHC (or future collider) observables. A numerical analysis of both approaches is of interest.

Look at:

- different orders
- scale variation uncertainties
- influence of non-perturbative factors

Z p_T at LL with reSolve

Use 9-point scale variation to estimate uncertainty from scale choices.

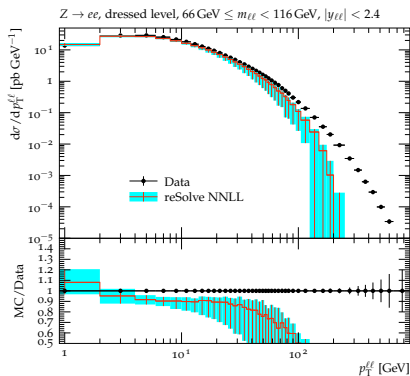
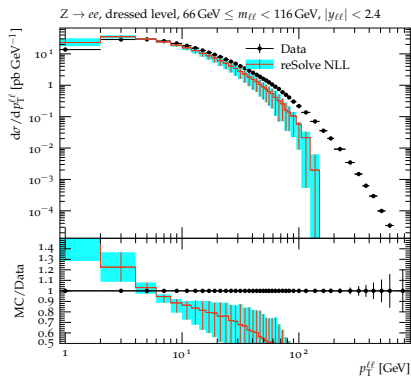


Leading logarithmic calculation

The hourglass shape of the uncertainty is due to:

- growing uncertainties at small p_T
- no (matching to) finite terms to describe large p_T region

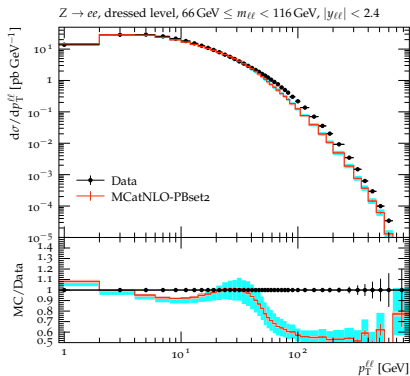
Z p_T at NLL and NNLL with reSolve



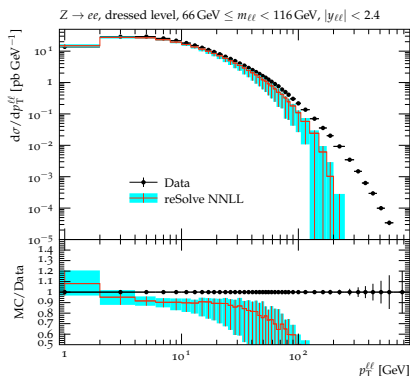
General observation: shape improves when going to NNLL. Uncertainties are smaller than in the LL prediction.

Comparison of Z boson p_T spectra

Compare result of PB TMD with reSolve result. Both with scale uncertainties.



MC@NLO ME matched to TMD in Cascade,
using PB TMD set2



CSS calculation at NNLL, no matching to finite
terms

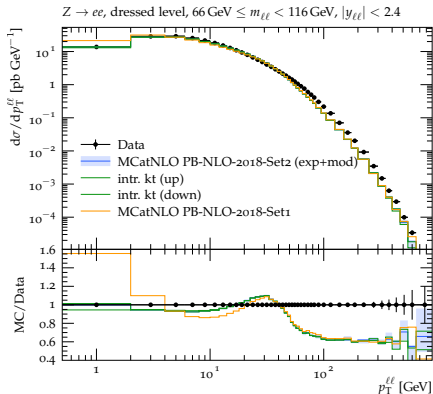
Non-perturbative parameterization

How is dealt with the non-perturbative contribution to TMDs?

Parton branching

- Intrinsic transverse momentum

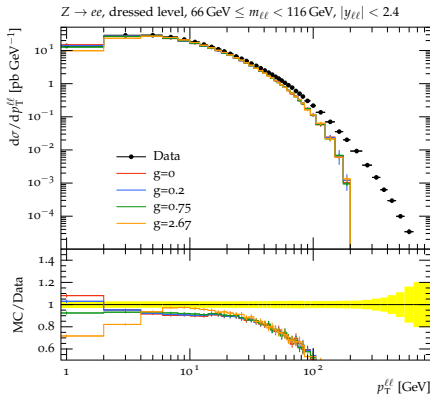
$$\tilde{\mathcal{A}}_a(x, k_\perp, \mu_0) = \tilde{f}_a(x, \mu_0) \exp\left(-\frac{k_\perp^2}{\sigma^2}\right)$$



[A. Bermudez Martinez et al.
arXiv:1906.00919v2]

CSS

- reSolve uses Gaussian smearing factor for large b : $\exp\{-g^{NP} b^2\}$



Summary

The PB approach for TMDs takes into account soft gluon emissions ($z \rightarrow 1$) and all transverse momenta (q_{\perp}) from branchings in the QCD evolution

- PB TMDs provide possibility to do calculations of **exclusive** observables, contrarily to semi-analytical calculations which are **inclusive**
- TMDs are applicable in the Cascade MC event generator where the parton shower matches the dynamics of the TMDs.
- Resummation of $\ln(Q^2/q_{\perp}^2)$ in the Sudakov up to NLL accuracy

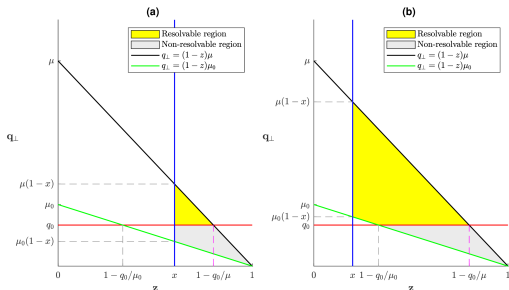
Future:

- fit TMDs with dynamical z_M to DIS and DY data
- applications to processes beyond color-singlet production, e.g. multi-jets

Back-up

PB: map evolution variable to transverse momentum

Change phase space variable μ' to q_{\perp} with angular ordering condition



- Evolution in q_{\perp} down to q_0 (Red line) for all z (case a)
- When $x < z < 1 - q_0/\mu_0$ (case b): $q_{\perp, \min} = (1-z)\mu_0$ (Green line)
 - ▶ Subtraction term arises in evolution equation:

$$\begin{aligned}
 \tilde{f}_a(x, \mu^2) &= \Delta_a(\mu^2, \mu_0^2) \tilde{f}_a(x, \mu_0^2) + \sum_b \int \frac{dq_{\perp}^2}{q_{\perp}^2} \int_x^1 dz \left[\Theta(q_{\perp}^2 - q_0^2) \Theta(\mu^2(1-x)^2 - q_{\perp}^2) \right. \\
 &\quad \times \Theta(1 - q_{\perp}/\mu - z) - \Theta(q_{\perp}^2 - q_0^2) \Theta(\mu_0^2(1-x)^2 - q_{\perp}^2) \Theta(1 - q_{\perp}/\mu_0 - z) \left. \right] \\
 &\quad \times \Delta_a \left(\mu^2, \frac{q_{\perp}^2}{(1-z)^2} \right) P_{ab}^{(R)}(z, \alpha_s(q_{\perp}^2)) \tilde{f}_b \left(\frac{x}{z}, \frac{q_{\perp}^2}{(1-z)^2} \right)
 \end{aligned} \tag{8}$$

Single emission \leftrightarrow multiple emission

	Multiple emission	Single emission
(z, μ')	CMW/PB	
(z, q_{\perp})	PB	KMRW

Kimber Martin Ryskin Watt (KMRW) approach constructs TMDs in a single step

[Kimber, Martin, Ryskin, Phys.Rev. D63 (2001) 114027]

[Watt, Martin, Ryskin, Eur.Phys.J. C31 (2003) 73-89]

[Martin, Ryskin, Watt, Eur.Phys.J. C66 (2010) 163-172]

$$\begin{aligned} \tilde{f}_a(x, \mu^2) &= T_a(\mu^2, \mu_0^2) \tilde{f}_a(x, \mu_0^2) \\ &+ \sum_b \int_{\mu_0^2}^{q_{\perp, M}^2} \frac{dq_{\perp}^2}{q_{\perp}^2} \left\{ \underbrace{T_a(\mu^2, q_{\perp}^2) \int_x^{1-C(q_{\perp}, \mu)} dz P_{ab}^{(R)}(z, \alpha_s(q_{\perp}^2)) \tilde{f}_b\left(\frac{x}{z}, q_{\perp}^2\right)}_{\text{TMD: } \tilde{f}_a(x, q_{\perp}^2, \mu)} \right\} \end{aligned} \quad (9)$$

[Golec-Biernat, Stasto, Phys.Lett. B781 (2018) 633-638], [Guiot, e-Print: arXiv:1910.09656]

Ordering condition sets cut-off in q_{\perp} and z integration

- Strong ordering (SO): $C(q_{\perp}, \mu) = \frac{q_{\perp}}{\mu}$, $q_{\perp, M} = \mu(1-x)$
- Angular ordering (AO): $C(q_{\perp}, \mu) = \frac{q_{\perp}}{q_{\perp} + \mu}$, $q_{\perp, M} = \frac{\mu(1-x)}{x}$

Comparison KMRW and PB

KMRW

$$\begin{aligned} \tilde{f}_a(x, \mu^2) &= T_a(\mu^2, \mu_0^2) \tilde{f}_a(x, \mu_0^2) \\ &+ \sum_b \int_{\mu_0^2}^{q_{\perp, M}^2} \frac{dq_{\perp}^2}{q_{\perp}^2} \int_x^{1-C(q_{\perp}, \mu)} dz T_a(\mu^2, q_{\perp}^2) P_{ab}^{(R)}(z, \alpha_s(q_{\perp}^2)) \tilde{f}_b\left(\frac{x}{z}, q_{\perp}^2\right) \end{aligned} \quad (10)$$

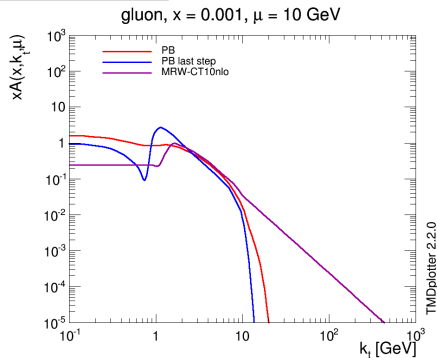
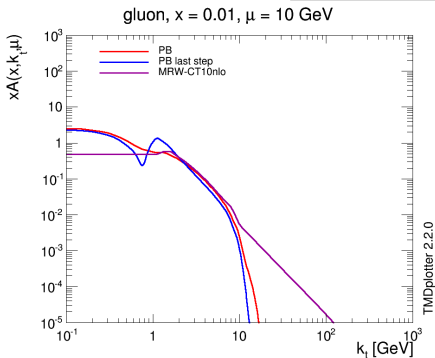
Parton branching (angular ordering & dynamic z_M)

$$\begin{aligned} \tilde{f}_a(x, \mu^2) &= \Delta_a(\mu^2, \mu_0^2) \tilde{f}_a(x, \mu_0^2) \\ &+ \sum_b \int_{q_0^2}^{\mu^2(1-x)^2} \frac{dq_{\perp}^2}{q_{\perp}^2} \int_x^{1-\frac{q_{\perp}}{\mu}} dz \frac{\Delta_a(\mu^2, \mu_0^2)}{\Delta_a\left(\frac{q_{\perp}^2}{(1-z)^2}, \mu_0^2\right)} P_{ab}^{(R)}(z, \alpha_s(q_{\perp}^2)) \tilde{f}_b\left(\frac{x}{z}, \frac{q_{\perp}^2}{(1-z)^2}\right) \end{aligned} \quad (11)$$

- KMRW has no rescaling in:
 - a) initial distributions \tilde{f}_b ,
 - b) Sudakov form factors $T_a \leftrightarrow \Delta_a$
- Differences in phase space limits (mostly pronounced in AO)

Numerical comparison: TMDs

Gluon TMD¹ versus k_{\perp} , $\mu = 10$ GeV



MRW-CT10nlo is KMRW TMD constructed from integrated PDF CT10nlo

- low k_{\perp} : bump at lower scale from single emission
- middle k_{\perp} : agreement KMRW and PB
- high k_{\perp} tail from radiative effects + Sudakov

¹PB last step is an invented way to simulate PB with a single emission

Colour coherence

Emitted transverse momentum in steps i and $i + 1$ equal to:

$$q_{\perp,i} = (1 - z_i) | k_{i-1} | \sin \theta_i \quad (12)$$

$$q_{\perp,i+1} = (1 - z_{i+1}) | k_i | \sin \theta_{i+1} \quad (13)$$

use $k_i/k_{i-1} = z_i$ so that:

$$\frac{q_{\perp,i+1}}{q_{\perp,i}} = \frac{(1 - z_{i+1})z_i | k_{i-1} | \sin \theta_{i+1}}{(1 - z_i) | k_{i-1} | \sin \theta_i} \quad (14)$$

$$\simeq \frac{(1 - z_{i+1})}{(1 - z_i)} z_i \frac{\theta_{i+1}}{\theta_i} \quad (15)$$

$$(16)$$

$$\frac{q_{\perp,i+1}(1 - z_i)}{(1 - z_{i+1})q_{\perp,i}} = z_i \frac{\theta_{i+1}}{\theta_i} \quad (17)$$

$$\frac{\bar{q}_{\perp,i+1}}{\bar{q}_{\perp,i}} = z_i \frac{\theta_{i+1}}{\theta_i} \quad (18)$$

Colour coherence results in subsequent emissions are ordered in their angle of emission: $\theta_{i+1} > \theta_i$.
Such that

$$\bar{q}_{\perp,i+1} > z_i \bar{q}_{\perp,i} \quad (19)$$